EEG Source Imaging: Correlate Source Locations and Extents with ECoG and Surgical Resections in Epilepsy Patients

Lei Ding[1], **Christopher Wilke**[1], **Bobby Xu**[1], **Xiaoliang Xu**[1], **Wim van Drongelene**[2], **Michael Kohrman**[2], and **Bin He**[1,*]

[1]University of Minnesota, Department of Biomedical Engineering

[2]University of Chicago, Department of Pediatrics

Abstract

It is desirable to estimate both location and extent information of epileptogenic zones from noninvasive EEG. In the present study, we use a subspace source localization method, i.e. FINE, combined with a local thresholding technique to achieve such tasks. We have evaluated the performance of this method in interictal spikes from three pediatric patients with medically intractable partial epilepsy. The present results suggest that the thresholded subspace correlation, which is obtained from FINE scanning, is a favorable marker, which implies the extents of current sources associated with epileptic activities. Our findings were validated through comparison to invasive ECoG recordings during interictal spikes. The surgical resections in these three patients are well correlated with the epileptogenic zones identified from both EEG sources and ECoG potential distributions. The value of the proposed noninvasive technique for estimating epileptiform activity was supported by satisfactory surgery outcomes.

Keywords

source localization; extent; EEG; ECoG; FINE; epilepsy; interictal; MRI; surgical outcome

It is clinically important to locate epileptogenic zones for patients with intractable epilepsy. The electrocorticogram (ECoG) recorded from subdural grid electrodes has become the 'gold standard' for defining epileptogenic zones (Engel et al., 1981) in clinical practice, although it is invasive and risky. The development of noninvasive techniques is much needed for the pre-surgical planning in patients with intractable epilepsy. An important question is whether such noninvasive techniques can provide as much information as the invasive ECoG.

The source imaging methods based on EEG or MEG have shown promise for noninvasive localization of epileptogenic zones using both interictal (Ebersole, 1994; Zhang et al., 2003) and ictal events (Lantz et al., 1999). Generally, EEG or MEG data from either interictal or ictal events are treated as a set of surface potential or magnetic field measurements produced by the equivalent sources associated with epileptic neural activations. The most basic brain electrical source model is the equivalent current dipole (ECD) (Scherg and von Cramon, 1985; He et al., 1987; Cuffin, 1995) which assumes that EEG or MEG signals are generated by one or a few focal currents. Each of the focal sources can be modeled by an ECD with parameters characterizing location, orientation, and moment (or strength). Many of them have been directly applied to the study of epileptic activities (Assaf & Ebersole, 1997; Ebersole, 1997;

*Correspondence: Bin He, Ph. D. University of Minnesota Department of Biomedical Engineering 7-105 Hasselmo Hall, 312 Church Street SE Minneapolis, MN 55455, USA E-mail: binhe@umn.edu.

Lantz et al., 1999; Assaf et al., 2003). However, in the ECD model, there is no parameter as a possible indicator of *source extent*, which is important for determining the area of tissue exhibiting epileptic behavior. Such *extent* information can possibly be characterized by source imaging methods based on the distributed source models (Hämäläinen and Ilmoniemi, 1984; Dale and Sereno, 1993; Pascual-Marqui et al., 1994; He et al., 2002a; Babiloni et al., 2005; Liu et al., 2006), which reconstructs current sources by finding the most probable current distribution that adequately explains the measured data (He & Lian, 2005). The source space usually covers the entire human brain and is represented by continuously distributed voxels, each of which stands for a local current source. The number of voxels (more than a couple of thousand) is normally significantly larger than the number of measurements (around 100), which makes the problem underdetermined (Dale and Sereno, 1993; He, 1999) and requires the use of prior constraints to regularize the inverse solution. Such constraints result in low resolution solutions. In order to estimate source extents, the solution found on the continuously distributed voxels can be thresholded (Darvas et al., 2004). The thresholding techniques have been developed and evaluated in computer simulations to decide optimal regularization parameter (Darvas et al., 2004) and to investigate different source localization methods with the distributed source models (Grova et al., 2006).

The objective of the present study is to investigate a high-resolution subspace source localization approach (first principle vectors, FINE) (Xu et al., 2004; Ding & He, 2006) in imaging the locations and estimating the extents of current sources from the scalp EEG of interictal events. The subspace source localization method was first introduced by Mosher et al. (1992) in MEG, and was known as multiple signal classification (MUSIC). The FINE method has demonstrated enhanced performance as compared with MUSIC and RAP-MUSIC for multiple closely located sources and sources of considerable coherence (Xu et al., 2004; Ding & He, 2006). The subspace source localization method is based on the dipole source model. However, it does not perform source localization by estimating the parameters used to characterize dipole sources. Rather, it scans the entire possible source space to obtain a metric for each scanned point, i.e. subspace correlation (SC), which indicates the variance of the dipolar pattern generated by the scanned point as explained by the scalp EEG measurements. The results from FINE is a tomography of SC values, which can be thresholded to estimate the extents of sources, such as, as suggested by a computer simulation study using a global thresholding technique (Darvas et al., 2004). Considering that the detection sensitivities of FINE for different neural sources are different due to their different configurations in location, orientation, and extent, we propose here a local thresholding technique to threshold the solution from FINE scanning in the present study. The performance of this proposed method was evaluated in three pediatric patients with medically intractable partial epilepsy. The noninvasive imaging results were evaluated by invasive subdural ECoG recordings and surgical outcomes in the same patients.

MATERIALS AND METHODS

Patients

Three pediatric patients with intractable epilepsy were studied using a protocol approved by the Institutional Review Boards of the University of Minnesota and the University of Chicago. The clinical studies took place at the Pediatric Epilepsy Center at The University of Chicago Children's Hospital. All patients had evaluations with structural MRI, long-term video EEG monitoring with scalp electrodes and subsequently with subdural electrodes. Following surgical resection, all patients are either seizure free or have had significant reduction of seizure occurrence.

Data acquisitions

EEG and ECoG—The scalp EEG data were obtained from 24 scalp electrodes, placed according to the 10-10 system (American Electroencephalographic Society, 1994) with a sampling rate of 400 Hz and band-pass filtering at 1-100 Hz (BMSI 6000, Nicolet Biomedical Inc., Wisconsin). The ECoG data from the same patients were recorded during postoperative monitoring from implanted subdural electrode arrays (e.g. 8×8, 8×4) or smaller strips (e.g. 8×1) (Radionics Medical Products Inc., Burlington, Massachusetts) placed directly on the cortex. The ECoG signals were digitized at 400 Hz and filtered with a 1-100 Hz band-pass filter.

MRI and CT—Each of the three patients received an MRI scan of the head before the surgical evaluation and two of them also had MRI scans after surgical resection. The T1-weighted MR images were obtained with a 1.5 Tesla scanner and were composed of 124 continuous coronal slices with 1.5 mm slice thickness. Each slice contained 256×256 pixels and the field of view (FOV) was 220×220 (mm). The CT images were obtained from the subjects and were composed of 116 continuous axial slices with slice thickness of 1.25 mm. Each slice contained 512×512 pixels and the FOV was 250×250 (mm).

EEG source estimation

Realistic head modeling and electrode co-registration—The boundary element (BE) model, which consisted of the scalp, skull, and brain surfaces, was constructed for each of the three patients by CURRY 4.5 (NeuroScan Lab, TX) using the preoperative MRI data. The conductivities of the scalp and brain were set to 0.33 $S·m^{-1}$ and the conductivity of the skull was set to 0.0165 $S·m^{-1}$ (Oostendorp et al., 2000; Lai et al., 2005).

The scalp electrode positions were measured with a 3D digitizer (Polhemus, Colchesterm, VT). The positions of the implanted subdural electrode arrays were decided from the CT images using segmentation tools from CURRY 4.5 (Zhang et al., 2006). The co-registration between the different imaging modalities, i.e. MR and CT, and between structure images with electrical recording sensors, i.e. scalp electrodes, was achieved by fiducial points (nasion, left, and right preauricular points) and a surface fitting algorithm (CURRY 4.5).

IIS selection—The EEG and ECoG records were reviewed for the occurrence of interictal spikes (IIS) by experienced epileptologists. Fig. 1, Fig. 3(a), and Fig. 4 (a) show the 24-channel scalp waveforms of IISs from patient #1, patient #2, and patient #3, respectively. The EEG was reformatted to an average reference montage for illustration and analysis. The peaks of the interictal were marked with red points on the channels with maximal signal strength. The time segment for each interictal data for subsequent spatio-temporal source imaging analysis of FINE was examined using a time-frequency representation (TFR) (Qin et al., 2004). The frequency bin with the maximal signal energy was identified from each TFR, which represented the average intensity over all electrodes. The temporal window was defined by the full width at half maximum (FWHM) principle at the identified frequency bin (Ding et al., 2006).

FINE—The FINE algorithm (Xu et al., 2004) is developed under the framework of the subspace source localization approach (Mosher et al., 1992) and solves the spatiotemporal source localization problem using a scanning procedure. The FINE method scans the entire possible source space and calculates the subspace correlation of two subspaces (Ding & He, 2006).

$$SC^2_{FINE}(\bar{r}) = \min_{\bar{q}} \left(\frac{A(\bar{r},\bar{q})^T F_\Theta F_\Theta^T A(\bar{r},\bar{q})}{A(\bar{r},\bar{q})^T A(\bar{r},\bar{q})} \right)$$

1

$A\left(\overline{r},\overline{q}\right)$ corresponds the subspace spanned by a particular scanned dipole source and F_{Θ} is the FINE vector set, which is a subset of the noise-only subspace. Sources can be found as those for which the scanning metric $SC^2_{FINE}\left(\overline{r}\right)$ is sufficiently close to zero (Xu et al., 2004; Ding & He, 2006; Ding et al., 2006). The procedure to find the noise-only subspace is based on the singular value decomposition (SVD) analysis of scalp EEG measurements (Ding et al., 2006). For each scanned point, the SC metric is optimized by selecting a unique subset from the noise-only subspace for each point to perform its calculation (Xu et al., 2004).

Local thresholding strategy—It is known that the scalp EEG has different sensitivities due to different source configurations, such as source location, orientation, extent, depth and strength. When sources with different configurations exist at the same time, the EEG signals should have different power contributions from different sources, which lead to different signal-tonoise ratios (SNR) during the real experimental recordings. In the FINE method, this fact indicates that the signals with lower powers in EEG, more contaminated by noise, have higher SC values against the FINE vector set. We thus set a conservative SC value threshold as 0.05. Any SC value below this threshold can be regarded as a possible source. Since a real source can make its neighboring points have low SC values, another criterion for a source is that the SC value of the point is a local minimum in the 3- dimensional tomography of SC, which actually indicates the gravity of a source.

To estimate the extent of a source, a local thresholding strategy is applied here.

$$1-(1-SC_{\min})\times R \qquad\qquad 2$$

where $SC_{\min}$ is the SC values for the sources of local minimum identified in the above described procedure. The local threshold for each source is calculated by increasing SC value with $SC_{\min}$ as a baseline by a certain ratio, R, which is same for all sources. However, because $SC_{\min}$ is different for different sources, the threshold values are different for different sources. This principle is applied to the neighboring points of each source to determine its extent.

RESULTS

Patient #1—Fig. 1 shows the preoperative scalp EEGs recorded from 24 electrodes of two typical IISs from patient #1. While the first IIS (Fig. 1 (a), left) shows strong activities in right frontal and right parietal lobes as well as activity in right lateral temporal lobe, the second IIS (Fig. 1 (b), left) has activity with more focal energy in the right lateral temporal lobe. One of the sources estimated by FINE for the first IIS is located in the right posterior temporal lobe and other two are located in the right frontal lobe (Fig. 1 (a), right). In the second IIS, two closely neighbored sources are found in the right anterior temporal lobe (Fig. 1 (b), right). As these plots only indicate the locations of the sources, Fig. 2 (a-b) (top) show the extents of these sources obtained using the local thresholding technique described in equation (2). The ECoG was recorded from five subdural electrode pads (Fig. 2 (a-b), left and right): one with 8×8 electrodes (only 40 were used for recording) covering the posterior inferior frontal lobe and the temporal lobe; one with 8×2 electrodes covering the inferior frontal lobe; one with 8×1 electrodes covering the gap between the inferior frontal lobe and the temporal lobe; one with 8×1 electrodes curving around the temporal tip; and one with 8×1 electrodes curving underneath the inferior temporal lobe heading medially. Fig. 2 (a-b) (left) also show subdural potential distributions (50% of maximum) at the peaks of two typical postoperative ECoG IISs, which are exactly corresponding to the EEG sources from FINE of two preoperative EEG IISs. By plotting them together (Fig. 2 (a-b), right), we can see they are consistent in location. Furthermore, the relative extent ratios between multiple activated areas (three for the first IIS and two for the second IIS) in the EEG sources are quite similar to the ratios from the ECoG

potentials. Note that the two sources from the second IIS are quite close, but their source extents show different orientations. This difference is also reflected in the ECoG potentials which show two intersected negative patterns with a certain angle. These results are also consistent with presurgical evaluations for this patient, who is diagnosed with epileptogenic zones in three areas: right frontal lobe (F), right anterior temporal lobe (AT), and right posterior temporal lobe (PT). The postoperative MRI (Fig. 2 (c), right) shows the locations for the resections of these areas (marked by red arrows). The cortex model (Fig. 2 (c), left) of the patient reconstructed from postoperative MRI shows the loss of cortical brain tissue in these three areas (also marked by red arrows). After resection, the seizures in this patient were significantly reduced.

Patient #2—The preoperative scalp EEG of a typical IIS from patient #2 shows strong activity in the right frontal lobe which extends to the right temporal and right parietal lobes (Fig. 3 (a), left). The EEG sources estimated by FINE are located in the right frontal parietal lobe (Fig. 3 (a), right) with two very close together and the other one more posterior. Fig. 3 (b) (top) shows the extents of these sources after local thresholding. Two anterior sources are fused together with a relative larger extent than the posterior source. The ECoG was recorded from six subdural electrode pads (Fig. 3 (b), left and right): one with 8×8 electrodes (only 32 have recording) covering the entire parietal lobe and the superior temporal lobe, one with 8×4 electrodes covering the inferior frontal lobe, one with 6×1 electrodes curving around the temporal tip, one with 8×1 electrodes curving underneath the inferior temporal lobe heading medially, and the last two with 8×1 electrodes each covering the temporal lobe laterally. Fig. 3 (b) (left) shows subdural potential distributions (60% of maximum) at the peak of the postoperative ECoG IIS, which are very consistent, in both location and extent (Fig. 3 (b), right), to the EEG sources found in the preoperative EEG IIS. The EEG source with larger extent also has the larger subdural potential extent in the ECoG recording while the smaller EEG source corresponds to the smaller subdural potential field. Note that the two neighbored negative peaks in ECoG for the anterior source may reflect the fact that the current source distribution in this source is due to two peaks which are fused together during local thresholding. These results are also consistent with presurgical evaluations for this patient,who is diagnosed with epileptogenic zones in the right frontal parietal lobe. After resection, the seizures in this patient were successfully eliminated.

Patient #3—The preoperative scalp EEG of a typical IIS from patient #3 shows strong activity in the right lateral parietal lobe (Fig. 4 (a), left) and the EEG source responsible for such observations is estimated to be located in the right medial temporal lobe (Fig. 4 (a), right). Fig. 4 (b) (top) shows the extent of the source after local thresholding. The ECoG was recorded from four subdural electrode pads (Fig. 4 (b), left and right): one with 8×8 electrodes covering the parietal lobe and the temporal lobe, one with 8×1 electrodes covering the temporal tip, one with 8×1 electrodes over the lateral temporal lobe, and the last one with 8×1 electrodes curving underneath the inferior temporal lobe heading medially. Fig. 4 (b) (left) shows the subdural potential distributions (50% of maximum) at the peak of the postoperative ECoG IIS. It is at the same location as the EEG source (Fig. 3 (b), right) found in the preoperative EEG IIS. The patient underwent right side medial temporal lobe resection as shown in the postoperative MRI and cortex model (Fig. 4 (c)), which resulted in the patient becoming seizure free.

DISCUSSION

The present study presents a method to estimate the locations and extents of epileptogenic zones from noninvasive scalp EEG in epilepsy patients with a subspace source localization method. The subspace source localization method is developed based on a dipole source model. Its unique scanning procedure allows us to estimate the extents of sources by the thresholding

techniques, which were only available for the source imaging solutions based on the distributed source model. The present results suggest that the thresholded subspace correlation is a good indicator of the extents of sources, which is revealed by the fact that the relative extents of multiple sources from a single EEG IIS are well correlated to the relative extents of multiple sources indicated by subdural ECoG potential distributions (in both patient #1 and #2). Further investigations are desirable to establish an evaluation concept on how to find a way to decide upon a thresholding value which is optimal and robust under different conditions. Potential solutions recently suggested by other researchers could possibly be achieved by receiver operating characteristic (ROC) curve (Darvas et al., 2004; Grova et al., 2006) or confidence volume (Fischer et al., 2005).

The thresholding performed in the present study used local threshold values for multiple sources occurring in a single IIS, which is different from the global thresholding techniques (Darvas et al., 2004; Grova et al., 2006). Each local threshold value of subspace correlation is decided by regarding the subspace correlation of the peak point as the baseline. This baseline reflects the sensitivity of the EEG and FINE solution to a specific source in multiple source localization problems. The different detection sensitivities in either EEG or FINE are due to the different current source configurations.

The estimation of current sources from preoperative EEG IISs are validated by the observations from postoperative ECoG IISs in the present study. The present results suggest that we are able to retrieve both location and extent information regarding current sources noninvasively. Although the IISs studied in EEG and ECoG are from different recording sessions, the consistency between the imaging results and postoperative ECoG recordings indicates the feasibility of correlating IIS sources in the same patients. More accurate validation study can be performed in a single IIS event with simultaneously recorded EEG and ECoG signals which is possible if the inhomogeneity introduced by the presence of low conductive ECoG pads can be successfully handled (Zhang et al., 2005). Our EEG findings are further evaluated by the surgical outcomes from three epilepsy patients. The resection areas are well correlated to the EEG source locations. Following surgical resection, two patients have become seizure free and one patient has had significant reduction of seizures.

The advantage of FINE is its ability in localizing multiple current sources. In the IISs we studied in the present work, FINE successfully identified multiple current sources in patient #1 (three sources for the first IIS and two sources for the second IIS) and patient #2 (three current sources). They are either separated by a couple of centimeters or are close (two sources for the second IIS in Patient #1 and two anterior sources among three in Patient #2). The ability of the FINE method to distinguish closely-located sources has been discussed and demonstrated in computer simulations and experimental studies (Ding and He, 2006). FINE is also an efficient spatio-temporal source localization method, which uses spatial and temporal data simultaneously by singular value decomposition. It detects the main activity patterns among the defined time windows and makes an entire fit over the whole temporal samples instead of individually at each time point. It is worthy to point out that FINE is able to image current sources over the 3- dimensional brain volume. It can estimate the depth information of current sources which may not be able to be obtained in ECoG, like in some adult epilepsy patients with deep epileptogenic zones.

In summary, we have developed a subspace source localization method to estimate locations and extents of epileptogenic zones and have tested its feasibility using interictal spikes from three pediatric patients with medically intractable partial epilepsy. The present results suggest that the thresholded subspace correlation, obtained from FINE scanning and thresholded by a local thresholding technique, may be a favorable indicator about the extents of current sources related to epileptogenic zones. Future investigations may optimize such an indicator under

various conditions, which would provide an important noninvasive means of estimating the locations and extents of epileptogenic zones from the scalp EEG measurements.

Acknowledgements

Reference

American Electroencephalographic Society. Guideline thirteen: guidelines for standard electrode position nomenclature. J. Clin. Neurophysiol 1994;11:111–3. [PubMed: 8195414]

Assaf BA, Ebersole JS. Continuous source imaging of scalp ictal rhythms in temporal lobe epilepsy. Epilepsia 1997;38(10):1114–23. [PubMed: 9579958]

Assaf BA, Karkar KM, Laxer KD, Garcia PA, Austin EJ, Barbaro NM, Aminoff MJ. Ictal magnetoencephalography in temporal and extratemporal lobe epilepsy. Epilepsia 2003;44(10):1320–27. [PubMed: 14510826]

Babiloni F, Cincotti F, Babiloni C, Carducci F, Basilisco A, Rossini PM, Mattia D, Astolfi L, Ding L, Ni Y, Cheng K, Christine K, Sweeney J, He B. Estimation of the cortical functional connectivity with the multimodal integration of high resolution EEG and fMRI data by Directed Transfer Function. Neuroimage 2005;24(1):118–31. [PubMed: 15588603]

Cuffin BN. A method for localizing EEG sources in realistic head models. IEEE Trans. on Biomed. Eng 1995;42:68–71.

Dale AM, Sereno MI. Improved localization of cortical activity by combining EEG and MEG with MRI cortical surface reconstruction: a linear approach. J. Cog. Neurosci 1993;5:162–76.

Darvas F, Pantazis D, Kucukaltun-Yildirim E, Leahy RM. Mapping human brain function with MEG and EEG: methods and validation. Neuroimage 2004;23:289–99.

Ding L, He B. Spatio-temporal EEG Source Localization Using a Three-dimensional Subspace FINE Approach in a Realistic Geometry Inhomogeneous Head Model. IEEE Trans. Biomedical Engineering, 2006;53(9):1732–9.

Ding L, Worrell GA, Lagerlund TD, He B. 3D Source localization of interictal spikes in epilepsy patients with MRI lesions. Physics in Medicine and Biology 2006;51(16):4047–62. [PubMed: 16885623]

Ebersole JS. Non-invasive localization of the epileptogenic focus by EEG dipole modeling. Acta. Neurol. Scand 1994;152:20–8.

Ebersole JS. Magnetoencephalography/magnetic source imaging in the assessment of patients with epilepsy. Epilepsia 1997;38(suppl 4):S1–5. [PubMed: 9240234]

Engel J, Rausch R, Lieb JP, Kuhl DE, Crandall PH. Correlation of criteria used for localizing epileptic foci in patient considered for surgical therapy of epilepsy. Ann. Neurol 1981;9:215–24. [PubMed: 7013652]

Fischer MJM, Scheler G, Stefan H. Utilization of magnetoencephalography results to obtain favourable outcomes in epilepsy surgery. Brain 2005;128:153–7. [PubMed: 15563514]

Grova C, Daunizeau J, Lina JM, Benar CG, Benali H, Gotman J. Evaluation of EEG localization methods using realistic simulations of interictal spikes. NeuroImage 2006;29:734–53. [PubMed: 16271483]

Hamalainen, MS.; Ilmoniemi, RJ. Interpreting measured magnetic fields of the brain: estimates of current distributions. Technical Report TKK-F-A559, Helsinki University of Technology: 1984.

He B. Brain electric source imaging: scalp Laplacian mapping and cortical imaging. Crit. Rev. Biomed. Eng 1999;27:149–88. [PubMed: 10864279]

He B, Musha T, Okamoto Y, Homma S, Nakajima Y, Sato T. Electric dipole tracing in the brain by means of the boundary element method and its accuracy. IEEE Trans. Biomed. Eng 1987;34:406–14. [PubMed: 3610187]

He B, Yao D, Lian J, Wu D. An equivalent current source model and Laplacian weighted minimum norm current estimates of brain electrical activity. IEEE Trans. Biomed. Eng 2002a;49:277–88. [PubMed: 11942719]

He B, Zhang X, Lian J, Sasaki H, Wu D, Towle VL. Boundary element method based cortical potential imaging of somatosensory evoked potentials using subjects' magnetic resonance images. NeuroImage 2002b;16:564–76. [PubMed: 12169243]

He, B.; Lian, J. Electrophysiological Neuroimaging. In: He, B., editor. Neural Engineering. Kluwer Academic/Plenum Publishers: 2005. p. 221-62.

Lai Y, van Drongelen W, Ding L, Hecox KE, Towle VL, Frim DM, He B. Estimation of in vivo human brain-to-skull conductivity ratio from simultaneous extra- and intra-cranial electrical potential recordings. Clinical Neurophysiology 2005;116:456–65. [PubMed: 15661122]

Lantz G, Michel CM, Seeck M, Blanke O, Landis T, Rosen I. Frequency domain EEG source localization of ictal epileptiform activity in patients with partial complex epilepsy of temporal lobe origin. Clin. Neurophysiol 1999;110:176–84. [PubMed: 10348337]

Liu Z, Keckman F, He B. Effects of fMRI-invisible Sources in EEG-fMRI Integrated Cortical Current Density Estimation: A Simulation Study. Clinical Neurophysiology 2006;117(7):1610–22. [PubMed: 16765085]

Mosher JC, Lewis PS, Leahy RM. Multiple dipole modeling and localization from spatiotemporal MEG data. IEEE Trans. On Biomed. Eng 1992;39(6):541–57.

Oostendorp TF, Delbeke J, Stegeman DF. The conductivity of the human skull: results of in vivo and in vitro measurements. IEEE Trans Biomed Eng 2000;47:1487–92. [PubMed: 11077742]

Pascual-Marqui RD, Michel CM, Lehmann D. Low resolution electromagnetic tomography: a new method for localizating electrical activity in the brain. Int. J. Psychophysiol 1994;18:49–65. [PubMed: 7876038]

Qin L, Ding L, He B. Motor Imagery Classification by Means of Source Analysis for Brain Computer Interface Applications. J of Neural Engineering 2004;1:135–41.

Scherg M, von Cramon D. Two bilateral sources of the late AEP as identified by a spatiotemporal dipole model. Electroencephalography & Clinical Neurophysiology 1985;62:32–44. [PubMed: 2578376]

Xu XL, Xu B, He B. An alternative subspace approach to EEG dipole source localization. Phys. Med. Biol 2004;49:327–43. [PubMed: 15083674]

Zhang X, van Drongelen W, Hecox K, Towle VL, Frim DM, McGee A, He B. High resolution EEG: cortical potential imaging of interictal spikes. Clinical Neurophysiology 2003;114:1963–73. [PubMed: 14499758]

Zhang YC, Ding L, van Drongelen W, Hecox K, Frim D, He B. Cortical potential imaging by means of the finite element method and its application to simultaneous extra- and intra-cranial electrical recordings. NeuroImage, 2006;31(4):1513–24. [PubMed: 16631381]
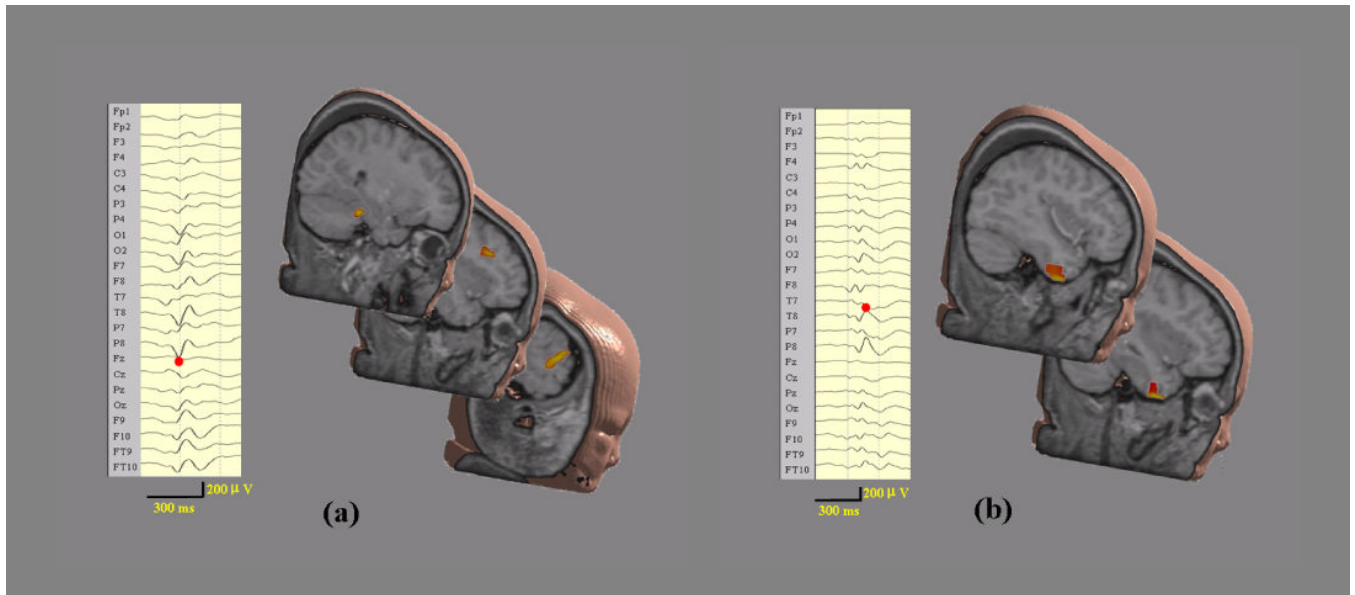
Figure 1.
Two IISs for Patients #1. (a) 24-channel waveforms of preoperative scalp EEG of the first IIS (Left); and EEG sources estimated by FINE (Right). (b) 24-channel waveforms of preoperative scalp EEG of the second IIS (Left); and EEG sources estimated by FINE (Right).
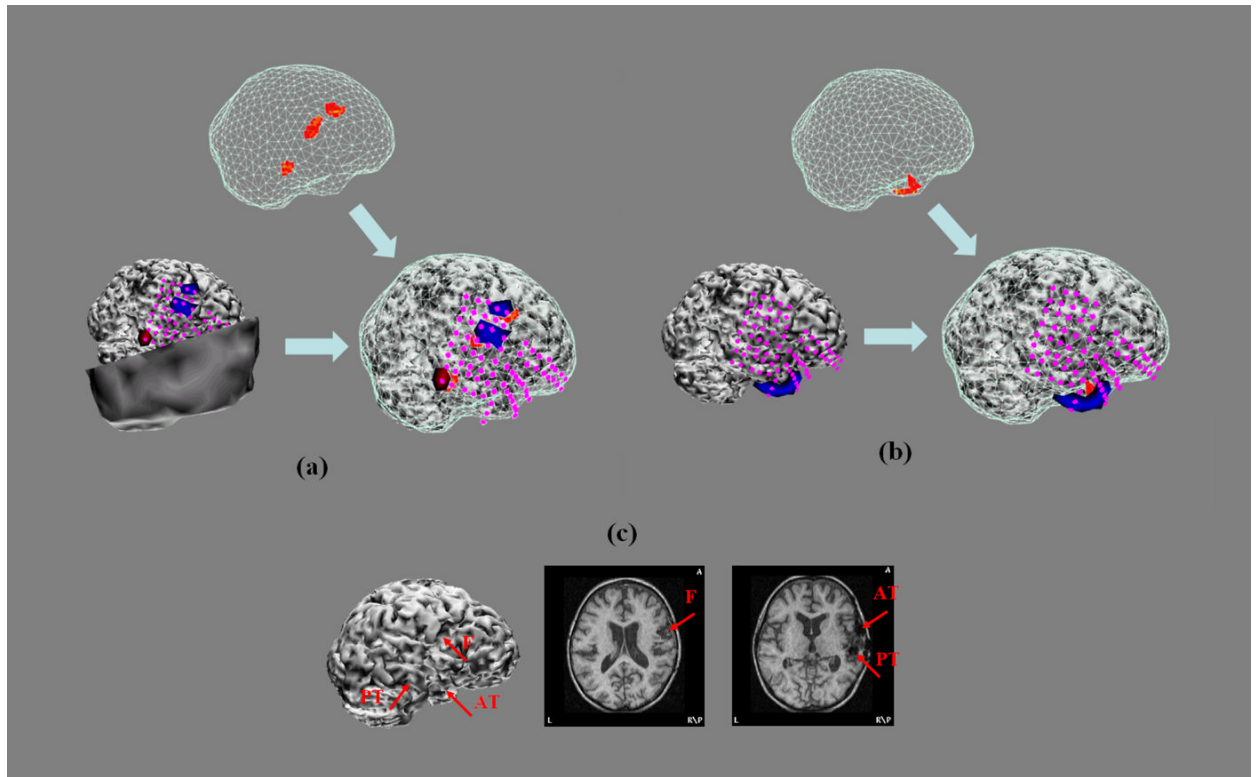
Figure 2.
Top: EEG sources from FINE shown by the scanned points with subspace correlation higher than local threshold values. Left: Potential distributions of postoperative ECoG recordings at the peak of an IIS. Magenta dots indicate the ECoG electrodes with recordings. Right: Co-registered plots of EEG sources (Top) and ECoG potentials (Left). (a) The first IIS for Patient #1. (b) The second IIS for Patient #1. (c) MRI after surgery resection of three areas (F: frontal; AT: anterior temporal; PT: posterior temporal).
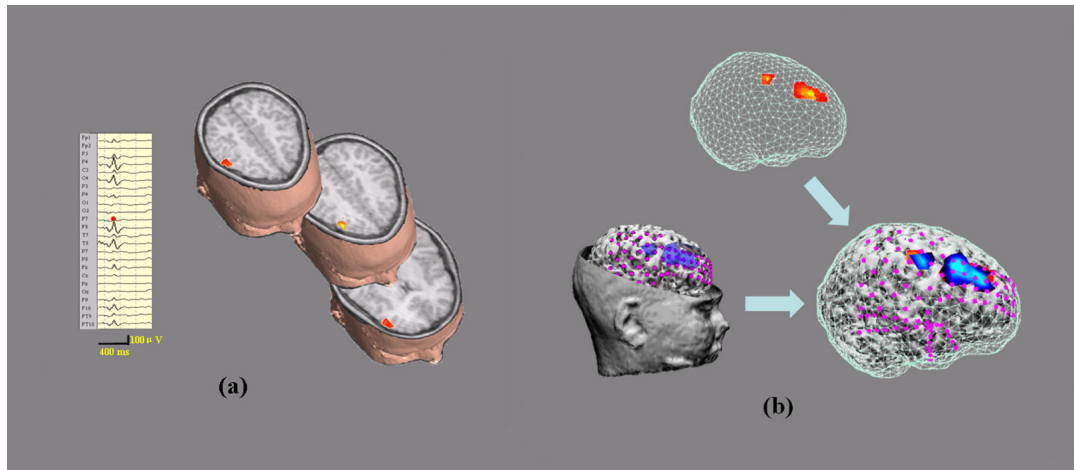
Figure 3.
(a) 24-channel waveforms of preoperative scalp EEG of an IIS for Patient #2 (Left); and EEG sources (Right). (b) Same as Fig. 2 (a) or (b).
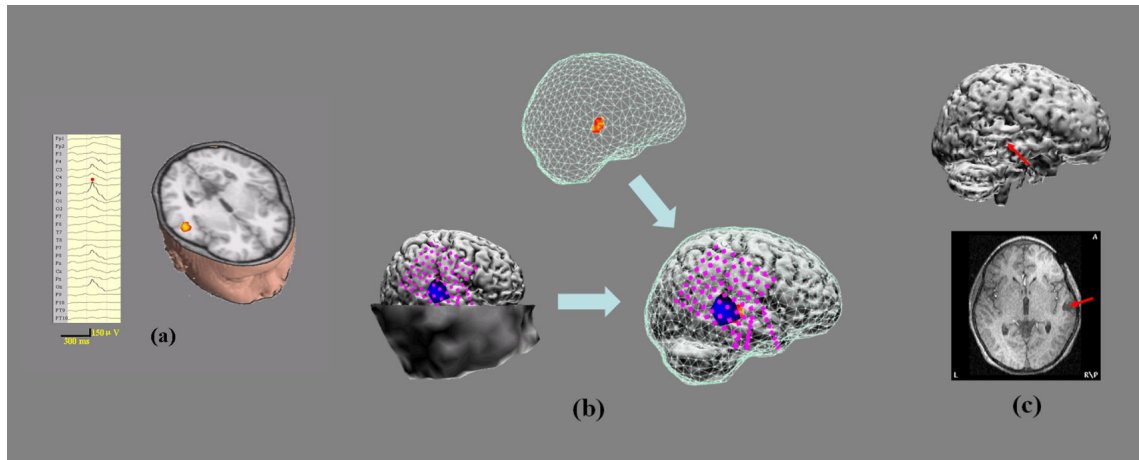
Figure 4.
(a) 24-channel waveforms of preoperative scalp EEG of an IIS for Patient #3 (Left); and EEG sources (Right). (b) Same as Fig. 2 (a) or (b). (c) MRI after surgery resection of medial temporal lobe.